

Separation of scattering and absorption in 1-D random media: II. Numerical experiments on stationary problems

Ru-Shan Wu* and Xiao-Bi Xie, *University of California, Santa Cruz*

SM5.3

SUMMARY

The theory of spatial distribution of seismic energy density in one dimensional (1D) random media derived in part I (Wu, 1993) is tested by numerical experiments using a full wave propagation matrix method. The geometry of numerical experiment mimics the configuration of zero-offset VSP (Vertical Seismic Profiling) along a borehole. A procedure of octave-band frequency averaging is applied to the measured data to reduce fluctuation of spatial energy distribution, so that stable estimations of medium parameters can be achieved without resorting to ensemble averaging. Results from Monte-Carlo numerical experiments for both infinite random media and finite random slabs with or without bottom reflections show good agreement for dark-to-gray (weak to intermediate scattering compared with absorption) media. When scattering is very strong (when backscattering-absorption ratio $S_b > 3$), results from single realization fluctuate substantially. However, most the practical situations of sedimentary rocks in the crust fall into the validity region of the energy transfer theory.

INTRODUCTION

In paper I (Wu, 1993, 1994), spatial distribution of seismic energy density and spatio-temporal distribution of seismic power in one dimensional (1D) random media have been derived using a phenomenological approach of energy transfer. The geometry of the formulation resembles the configuration of zero-offset VSP (Vertical Seismic Profiling) along a borehole. The theoretical treatment is complete for the case of 1D random media. It includes anisotropic scattering, finite thickness of a random slab and the influence of the bottom reflection of the slab. However, the energy transfer approach neglects totally the wave phenomena and therefore is only an approximate theory. In order to test the validity and the limitation of the theory, in this paper, we will compare the theory in paper I with numerical experiments based on full wave equation. Propagation matrix method is adopted as the numerical algorithm. We will concentrate on the stationary problem, namely the spatial distribution of seismic energy density, for infinite and finite random slabs with or without slab-bottom reflection.

SUMMARY OF THE THEORY

In the case of infinite 1D random media, assuming a point source is located at $z = 0$, the normalized seismic energy density $E_n(z) = 2E(z)/E_0$, where $E(z)$ is the measured energy density and E_0 is the source energy, is expressed as

$$E_n(z) = \sqrt{1 + 2S_b} \exp(-\sqrt{1 + 2S_b} \eta_a |z|) \quad (1)$$

where S_b is the backscattering-absorption ratio (B-A ratio), defined as

$$S_b = \eta_s^b / \eta_a \quad (2)$$

with η_s^b and η_a as the backscattering coefficient and absorption coefficient, respectively. S_b can be related with seismic albedo

B_0 (Wu 1993). For a finite random slab of thickness L with its top ($z = 0$) as free surface and a bottom reflection coefficient r_L , and assuming a point source is situated at $z = 0$ beneath the free surface, the total energy density can be calculated by the method of multiple-scattering series

$$E(x) = E^+(z) + E^-(z) = \sum_{m=0}^{\infty} E_m^+(z) + \sum_{m=0}^{\infty} E_m^-(z) \quad (3)$$

with

$$E_0^+(z) = E_0 G_b(z) \quad (4)$$

$$E_0^-(z) = 0 \quad (5)$$

$$E_m^+(z) = \int_0^z \eta_s^b E_{m-1}^-(z') G_b(z-z') dz' + \int_0^L \eta_s^b E_{m-1}^+(z') G_b(z+z') dz' \quad (6)$$

$$E_m^-(z) = \int_z^L \eta_s^b E_{m-1}^+(z') G_b(z-z') dz' + r_L \int_0^L \eta_s^b E_{m-1}^-(z') G_b(2L-z-z') dz' \quad (7)$$

where

$$G_b(z) = e^{-\eta_e^b |z|}, \quad (8)$$

is the Green's function with $\eta_e^b = \eta_a + \eta_s^b$ as the effective extinction coefficient, and E^+ and E^- are the forward and backward energy flux densities, respectively.

The energy summation series is monotonous and converges fast for realistic models. Each term of the series needs the same amount of calculation. Therefore the summation is easy to carry out. The energy density outside the random slab ($z > L$) can be calculated based on the obtained forward energy density at the slab bottom $E^+(L)$

$$E(z) = (1 - r_L) E^+(L) e^{-\eta_a(z-L)} \quad (9)$$

NUMERICAL EXPERIMENTS

Generation of 1D random media and wave propagation algorithms. Based on measurements from well-log data in the regions of sedimentary layers (Godfrey et al. 1980; Banik et al., 1985; Walden and Hosken, 1985; White et al., 1990), we assume an exponential correlation function with correlation length $a = 5m$ as our basic model of 1D random media, although the theory is independent of random medium spectra. Since the backscattering coefficient η_s^b is directly related to the power spectrum of scattering potential $\zeta = n^2 - 1$ (equation 10), we specify a random medium by giving its $P_\zeta(K)$. Fig. 1 shows an example of such a random medium of exponential correlation function with RMS velocity perturbation of 10%. For very strong velocity perturbations ($\epsilon > 10\%$), The resultant velocity profile may have some unreasonable extremes, with even negative values. Therefore, we cut the velocity values which deviate from the mean by more than 2 standard deviations for models with $\epsilon > 10\%$. The

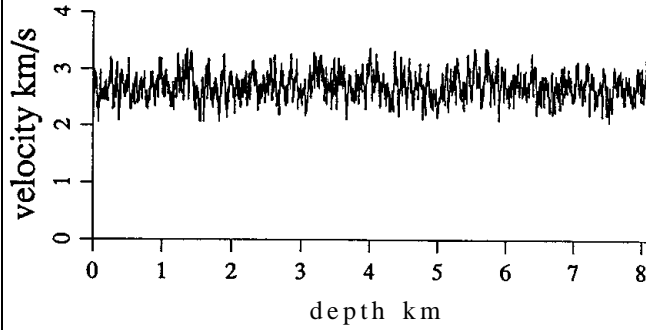


Figure 1: Velocity model of a 1D random medium having mean velocity of 3 km/s, RMS velocity perturbation $\epsilon = 10\%$ and exponential correlation function with correlation length $a = 5$ m.

numerical method used is a full-wave propagation matrix method and therefore the synthetic seismograms include all multiple scattering and wave interference phenomena. This method has been used in the literature to simulate wave propagation in 1D random media (Richards and Menke, 1983; Tang and Burnes, 1992). Absorption is handled by introducing complex wavenumbers. To make the result causal, a slight velocity dispersion is introduced according to the absorption-dispersion relation. In the simulations, a point source with a pulse source time function (white spectrum) is put just below the free surface at $z = 0$. Receivers are collocated along z -direction. For most cases, the wave field at each receiver is calculated in the frequency domain with total 512 frequencies and an interval of $1/2.56$ Hz. Therefore the Nyquist frequency is 100 Hz.

Calculation of Scattering Coefficient in 1D Random Media. In the 1D case, scattering coefficient is defined as the scattered power in the forward or backward direction by a unit length heterogeneities for a unit incident power flux. Therefore, scattering coefficient is related to the strength and distribution of heterogeneities in the medium. In our treatment, only the backscattering coefficient η_s^b enters into the energy balance equation. It can be derived directly from the wave equation that

$$\eta_s^b = k_0^2 P_\zeta(2k_0)/4 \quad (10)$$

where $P_\zeta(K)$ is the power spectrum of the scattering potential $\zeta = n^2 - 1 = (v_0/v)^2 - 1$ and $k_0 = \omega/v_0$ with v_0 as the background velocity. When $\delta n \ll 1$, above equation becomes

$$\eta_s^b = \epsilon^2 k_0^3 P(2k_0) \quad (11)$$

where $\epsilon = \langle (\delta v/v_0)^2 \rangle^{1/2}$ is the relative RMS velocity perturbation of the random medium and $P(K)$ is the normalized power spectrum or "shape spectrum" of the random medium.

Octave-Band Frequency Averaging The multiple scattering process in the energy transfer approach neglects the wave interference and assumes incoherency between forward and backward scattered energy flux, so that the addition of wave energy fluxes at each point in the medium can be applied. For a monochromatic wave field the energy distribution along propagation path will have very strong fluctuation. The fluctuation can be reduced by taking ensemble average of the results from a sufficient number of realizations. For a single realization of random medium,

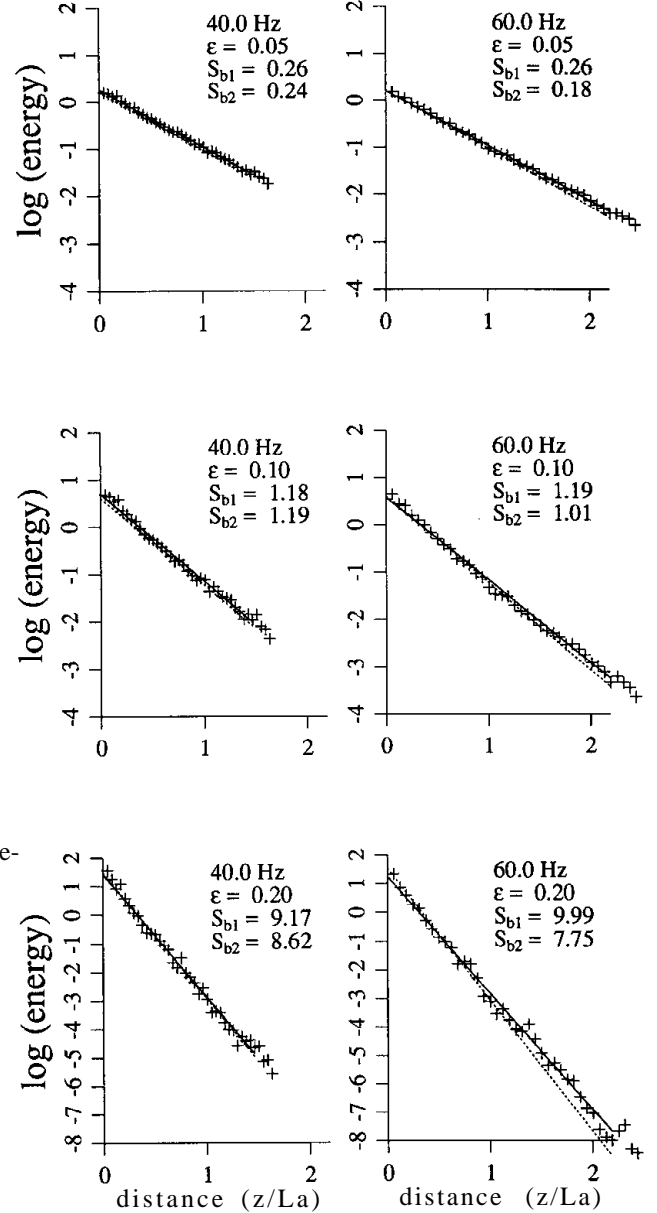


Figure 2: Energy distribution along propagation path in infinite random media for different frequencies with 2/3 pass-band averaging. Crosses are the measured values averaged over 10 realizations and solid lines are their least square fits. Dotted lines are the theoretical predictions. The top, middle and bottom figures are for weak, intermediate and strong scatterings, respectively. S_{b1} is the S_b value calculated directly from the medium η_s^b and η_a averaged over the passband; S_{b2} is that obtained from the inversion of measured energy distributions (solid lines).

the fluctuation can be reduced by frequency pass-band averaging. From Parseval theorem, we know that this pass-band power spectra summation is equivalent to the time domain integration of pass-band filtered seismograms. This is consistent with the requirement of energy transfer approach. However, the basic parameters of wave-medium interaction such as the absorption and scattering coefficients, are defined for monochromatic waves. Therefore, the match between the theory and observation with energy transfer approach can not be pushed to an arbitrary accuracy for a real medium (a single realization of a random medium). There is some fundamental limitation in this approach similar to the uncertainty principle. We will use the common practice for band-limited seismic waves as the compromise of the two conflict requirements. The pass-band is $2/3$ of the central frequency. This octave-band averaging is like a wavelet-packet decomposition of seismograms. In this way the frequency and time localizations (resolutions) vary with frequency and the wavelet for each frequency has a width of approximately one cycle of central frequency.

Results of Numerical Experiments The model is a 1D exponential random medium with correlation length $a = 5$ m. The average (background) velocity used is around 3 km/s, and the constant Q-factor is 200. The total length is 8.192 km with a sampling interval of 1 m. In order to simulate the multiple scattering for infinite medium, we put receiver only in the range of 0 - 4 km (total 40 receivers with interval of 0.1 km) to avoid the influence of bottom leakage.

In Fig. 2 results of energy distributions averaged over 10 realizations are given for the cases of weak, intermediate and strong scatterings ($\epsilon = 5\%$, 10% and 20%), respectively. In the figures, dotted lines are theoretical predictions (from equation 1), crosses are measured values from numerical experiments, and solid lines are the least-square linear fits of the measured values. The cen-

tral frequencies used here are 40 and 60 Hz. S_{b1} is the S_b value calculated directly from the medium η_s^b and η_a averaged over the passband; S_{b2} is that obtained from the inversion of measured energy distributions (solid lines). The agreement between theory and simulations are generally well. However, the disagreement becomes larger for strong scattering (bright media).

In order to see the statistical stability of the agreement, In Fig. 3 we plot the statistics of comparison between theory and simulations for the cases of one realization (Fig. 3a) and 10 realizations (Fig. 3b). Here the Q-factors used are 200 and 400, and the frequencies, 40, 50, 60 and 70 Hz. In the figures, horizontal axes are for true S_b , while the vertical ones, measured S_b from simulation. It can be seen that the agreement between theory and experiment deteriorates with the increase of velocity perturbations. In Fig. 3a the crosses are from single realizations. The shaded circles and pairs of bars are the means and standard deviations of the measured values for different S_b 's, respectively. The diagonal line (dotted) representing the perfect match is plotted as references. Fig. 3b shows the corresponding results for the case of 10 realizations, where crosses are the estimated S_b 's using only the decay slopes of energy distributions, while circles are those using both slope and intercept parameters. We see not only fluctuation but also some systematic bias of S_b estimation from predictions of the energy transfer theory for very strong scattering. However, this very strong scattering regime is beyond the range of most geophysical applications.

Fig. 4 shows the comparison between theory (dotted lines) and the averaged results of 10 realization simulations for a random slab of 1 km thick and located just below the free surface. The background velocity at the slab bottom jumps from 3 km/s to 4 km/s. The intrinsic Q is 200 for all frequencies. The top, middle and bottom figures are for weak, intermediate and strong scattering, respectively. In general, the simulations match the theory very well.

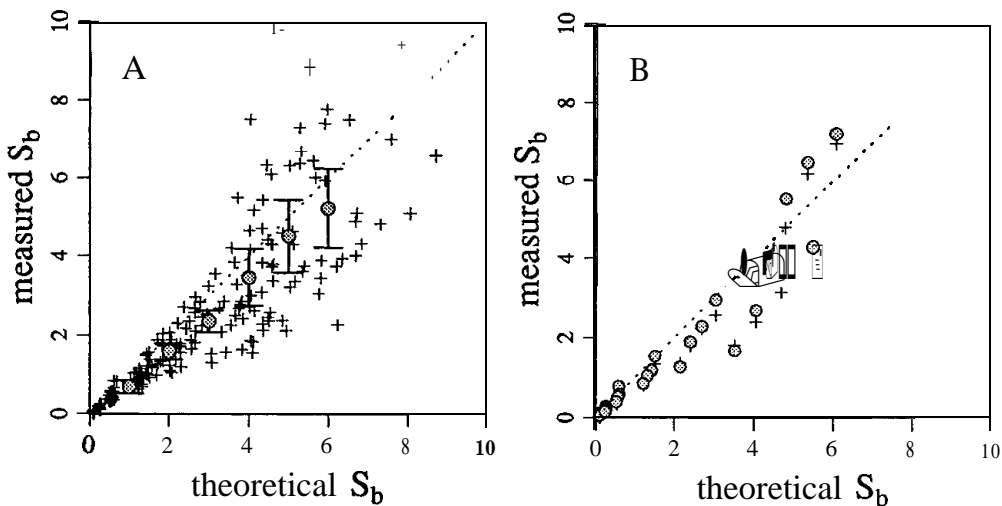


Figure 3: Stability of S_b estimation as a function of brightness S_b : (a). Results from single-realizations. Each cross is the estimate from the inversion of measured data for a single-realization of the random medium. The shaded circles and pairs of bars are the means and standard deviations, respectively. (b). Results from the average of 10 realizations. The crosses are for estimates using only energy distribution slopes; while the shaded circles are those using both intercepts and slopes of energy distribution curves.

CONCLUSION

It is demonstrated that for dark-to-gray (weak to intermediate scattering compared with absorption) media, i.e. when the brightness S_b of the medium is less than 2-3, spatial energy distribution predicted by the theory fits numerical experiments reasonably well for single-realizations of random media. When scattering is very strong ($S_b > 3$), results from numerical experiments fluctuate substantially. However, most sedimentary rocks in the Crust fall into the validity region of the energy transfer theory. The case of very bright medium (very strong scattering with little or no absorption) may be studied by full wave stochastic theory.

Since the seismic brightness S_b in typical exploration-seismological environments is in the range of 0.5 - 3, the apparent attenuation of primary waves will be affected strongly by scattering. Measurement of Q without considering the scattering influence will be seriously biased. The 1D energy transfer theory developed in paper I and the corresponding procedure of measurement presented in this work provide a viable method for solving this problem.

ACKNOWLEDGEMENTS

This work is supported partly by the NSF grant EAR-9205830 of USA and partly by a grant from the Los Alamos National Laboratory Institutional Supported Research Program, under the auspices of the United States Department of Energy.

REFERENCES

Banik, N.C., Lerche, I., Resnick, J.R. and Shuey, R.T., 1985, Stratigraphic Filtering, Part II: Model Spectra: *Geophys.*, 50, 2775-2783.

Godfrey, R., Muir, F., and Rocca, F., 1980, Modeling seismic impedance with Markov chains: *Geophysics*, 45, 1351-1372.

Richards, P.G., and Menke, W., 1983, The apparent attenuation of scattering medium: *Bull. Seis. Soc. Am.*, 73, 1005-1021.

Tang, X., and Burns, D.R., 1992, Seismic scattering and velocity dispersion due to heterogeneous lithology: Extended Abstract of SEG 62nd Annual meeting, 824-827.

Walden, A.T., and Hosken, J.W.J., 1985, An Investigation Of The Spectral Properties Of Primary Reflection Coefficients, *Geophys. Prospecting*, 33, 400-435.

White, B., Sheng, P., and Nair, B., 1990, Localization and backscattering spectrum of seismic waves in stratified lithology: *Geophysics*, 55, 1158-1165.

Wu, R.S. 1993, Separation of scattering and absorption in 1D random media from spatio-temporal distribution of seismic energy, Expanded Abstracts of the Technical Program, SEG 63th Annual Meeting, 1014-1017.

Wu, R.S., 1994, Spatial and temporal energy distributions of multiple-scattered waves in 1D random media and the separation of scattering from absorption. - I. theory: Submitted to *Geophysics*.

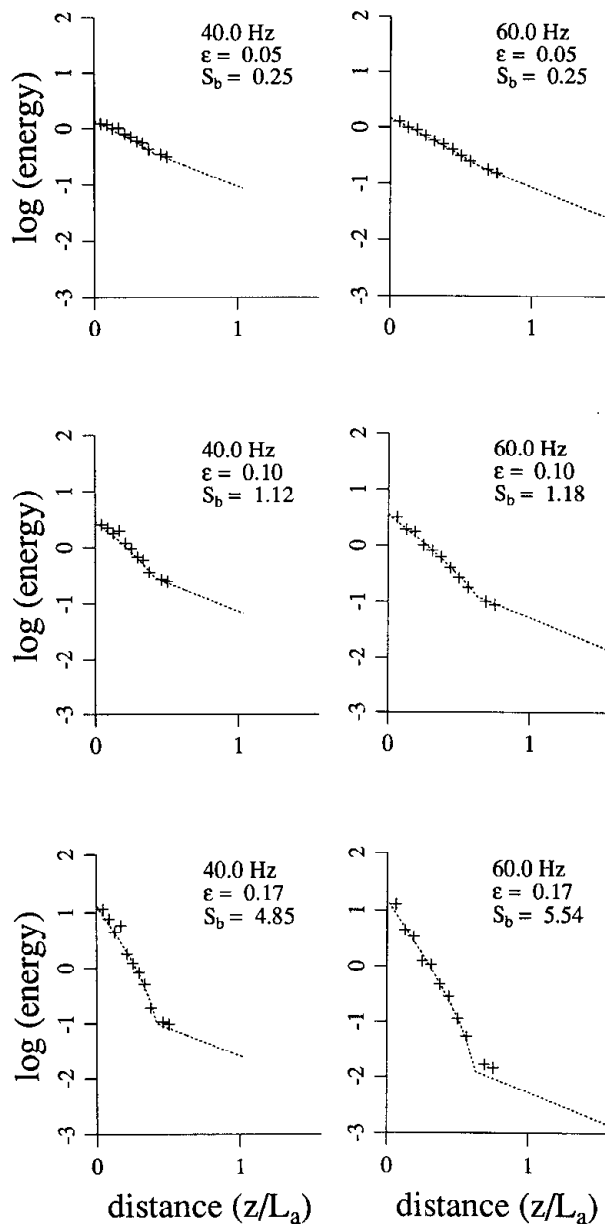


Figure 4: Energy distribution along propagation path in a finite random slab ($a = 5$ m) for different frequencies with $2/3$ pass-band averaging. The thickness of the slab is 1 km. The background velocity jumps from 3 km/s to 4 km/s at the bottom of the slab. The crosses are the measured values averaged over 10 realizations and the dotted lines are the theoretical predictions. The top, middle and bottom figures are for weak, intermediate and strong scatterings, respectively.